Field-Validated Multi-Bearing MCSA for Motor-Driven Pump Diagnostics and Maintenance Decision Support

Diego Cardona
Industrial Motor and Pump Diagnostics Project
Email: diego.cardonaparra@gmail.com

Field Test Collaborators
Excel Valencia Motor-Pump Test Campaign

***Abstract*—Motor Current Signature Analysis (MCSA) enables non-intrusive monitoring of motor-driven rotating equipment by extracting mechanical, electrical, and hydraulic fault information from stator-current signals. This paper presents a field-validated MCSA application for industrial centrifugal pump monitoring. The application uses synchronized three-phase acquisition, 32 kSPS waveform captures, high-resolution full-band FFT processing, and JSON-defined bearing geometry. The method evaluates drive-end (DE) and non-drive-end (NDE) bearings independently, reports BPFO/BPFI harmonic corroboration at first, second, and third defect harmonics, exposes fifth-harmonic pump sideband evidence, and converts spectral evidence into maintenance actions. The approach was evaluated on 53 field captures from a 10 HP motor-driven pump test campaign. The final report identified five maintenance-relevant captures at the beginning of the report: two requiring inspection of both bearings, two requiring drive-end inspection, and one routine monitoring recommendation. These evidence layers were added without changing the previously validated fault thresholds. The results show that explainable, multi-bearing MCSA can move beyond binary fault indication toward maintenance-oriented decision support.**

***Index Terms*—Motor Current Signature Analysis, MCSA, centrifugal pump, bearing fault diagnosis, BPFO, BPFI, predictive maintenance, FFT, condition monitoring.**

I. Introduction

Industrial centrifugal pumps are critical in water treatment, desalination, petroleum, process industries, and manufacturing. Traditional condition monitoring often relies on vibration sensors, acoustic measurements, or manual inspection. In many field installations, direct mechanical instrumentation is difficult, expensive, unsafe, or impractical. MCSA provides a practical alternative because stator currents can be measured from the control cabinet while still carrying signatures of load torque oscillations, rotor asymmetry, bearing defects, and pump hydraulic disturbances.

Recent work has demonstrated the value of current-based monitoring for centrifugal pump systems, bearing faults, impeller clogging, electrical submersible pumps, and cavitation/off-design operation. However, many practical systems still provide only binary fault indicators or single-frequency alarms. This is not enough for maintenance teams that must decide which component to inspect, when to inspect it, and how confident the evidence is.

This paper presents a field-oriented MCSA application that preserves classical MCSA interpretability while adding multi-bearing evidence, harmonic corroboration, grid-harmonic confidence metadata, and maintenance actions.

A. Contributions

The main contributions are:

1) independent DE and NDE bearing evaluation using geometry-specific BPFO/BPFI/BSF/FTF frequencies;
2) harmonic corroboration using $1\times$, $2\times$, and $3\times$ BPFO/BPFI evidence;
3) fifth-harmonic pump sideband evidence at $5f_0 \pm f_{mec}$;
4) grid-harmonic contamination evidence for interpreting candidate lines near nf_0;
5) a maintenance recommendation layer that prioritizes inspection and monitoring actions.

II. Related Work

Pump current analysis has been studied for explainable fault diagnosis, bearing defect detection, impeller clogging, electrical submersible pump monitoring, and cavitation detection. Prior work supports the central premise that mechanical and hydraulic phenomena can modulate motor current. The present work differs by focusing on a field application that reports multiple bearing locations, exposes harmonic corroboration, and translates spectral evidence into explicit maintenance actions.

III. System Architecture

The diagnostic application processes raw waveform captures with synchronized current and voltage channels sampled at $f_s = 32$ kSPS. The reference current channel is processed using high-resolution full-band FFT analysis. Runtime configuration is loaded from DSP, meter, calibration, and bearing-geometry files. The output is a structured JSON diagnostic record and a maintenance report.

IV. Mathematical Foundations

A. Bearing Characteristic Frequencies

For a rolling-element bearing with Z rolling elements, rolling-element diameter D_w, pitch diameter D, contact angle

TABLE I
LITERATURE THEMES COMPARED WITH THE FIELD APPLICATION.

Topic	Common treatment in literature	This application
Current-only monitoring	Feasibility shown for pumps and ESP assets	Implemented in an industrial waveform pipeline
Bearing frequencies	BPFO/BPFI/BSF/FTF from geometry	DE and NDE evaluated independently
Harmonic evidence	Often discussed, not always structured	$1\times$, $2\times$, $3\times$ BPFO/BPFI exported per bearing
Impeller disturbance	Sidebands near supply and fifth harmonic reported	$5f_0 \pm f_{mec}$ exported as pump evidence
Cavitation	Broad-band or energy-distribution phenomenon	Treated as band-energy behavior, not a single line
Decision support	Fault labels or severity scores	Explicit actions: inspect both, inspect DE, monitor
Grid harmonic contamination	Rarely explicit	Candidate frequencies annotated with nearest nf_0

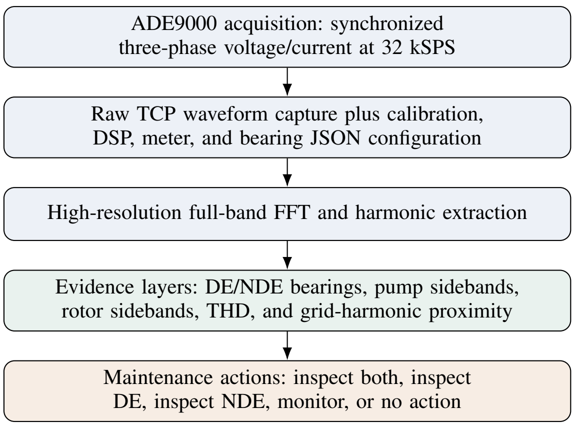

Fig. 1. MCSA application architecture from acquisition to maintenance recommendation.

α, and mechanical rotational frequency f_{mec}, the characteristic defect frequencies are

$$f_{BPFO} = \frac{Z}{2} f_{mec} \left(1 - \frac{D_w}{D} \cos\alpha\right), \tag{1}$$

$$f_{BPFI} = \frac{Z}{2} f_{mec} \left(1 + \frac{D_w}{D} \cos\alpha\right), \tag{2}$$

$$f_{BSF} = \frac{D}{2D_w} f_{mec} \left[1 - \left(\frac{D_w}{D} \cos\alpha\right)^2\right], \tag{3}$$

$$f_{FTF} = \frac{1}{2} f_{mec} \left(1 - \frac{D_w}{D} \cos\alpha\right). \tag{4}$$

The field bearing configuration contains two bearings: a drive-end 6309 and a non-drive-end 6206. The application evaluates every configured bearing independently.

B. Rotor and Pump Frequencies

Rotor broken-bar sidebands are evaluated around the fundamental frequency f_0 as

$$f_{BB} = f_0 \pm 2sf_0, \tag{5}$$

where s is per-unit slip. The mechanical blade-pass frequency is

$$f_{BPF} = N_b f_{mec}, \tag{6}$$

where N_b is the number of impeller blades. The monitored current sidebands appear around the electrical carrier as

$$f_{blade} = f_0 \pm N_b f_{mec}. \tag{7}$$

The pump evidence also exposes

$$f_{5H} = 5f_0 \pm f_{mec}, \tag{8}$$

which is used as corroborative evidence rather than as an independent fault trigger.

TABLE II
PER-BEARING SEVERITY LABELS.

B_{max} range	Severity
$B_{max} < 0.001$	none
$0.001 \le B_{max} < 0.003$	monitor
$0.003 \le B_{max} < 0.006$	warning
$B_{max} \ge 0.006$	alarm

V. METHOD

A. Multi-Bearing Evidence

Let $\mathcal{B} = \{b_1, b_2, \ldots, b_M\}$ be the set of configured bearings. For each bearing b_i, the application computes

$$\mathbf{f}_{b_i} = [f_{BPFO,i}, f_{BPFI,i}, f_{BSF,i}, f_{FTF,i}]. \tag{9}$$

A spectral extraction function $R(f)$ returns a normalized amplitude ratio at a target frequency. Per-bearing evidence is defined as

$$B_{max,i} = \max\left(R(f_{BPFO,i}), R(f_{BPFI,i})\right). \tag{10}$$

BSF and FTF are reported but excluded from B_{max} because field data showed higher susceptibility to unrelated mechanical and slip-related components.

B. Severity and Flagged Bearings

The severity label is assigned from $B_{max,i}$ using Table II. A bearing is included in the flagged list when its severity is warning or alarm. The list may contain no bearing, DE, NDE, or both.

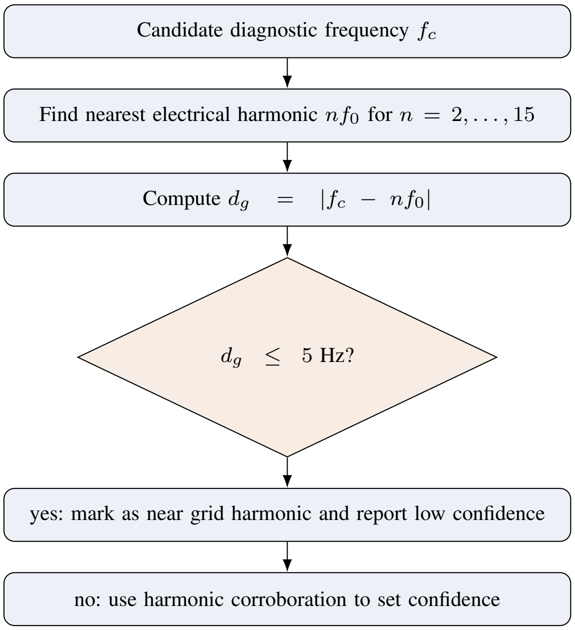

Fig. 2. Grid-harmonic contamination evidence for candidate diagnostic frequencies.

C. Harmonic Corroboration

For each bearing, additional evidence is extracted at

$$\mathcal{H}_{BPFO} = \{f_{BPFO}, 2f_{BPFO}, 3f_{BPFO}\}, \tag{11}$$

$$\mathcal{H}_{BPFI} = \{f_{BPFI}, 2f_{BPFI}, 3f_{BPFI}\}. \tag{12}$$

The harmonic count is

$$HC = \sum_{k=1}^{3} \mathbb{1}\left(R(kf_c) > \Gamma_k\right), \tag{13}$$

where f_c is BPFO or BPFI and Γ_k is the dynamic local noise-based gate. In this phase, HC is informational and does not modify the original bearing fault flag.

D. Grid-Harmonic Contamination Evidence

A key field observation was that diagnostic frequencies can lie close to electrical harmonics. For a candidate diagnostic frequency f_c, the nearest grid harmonic is

$$n^* = \arg \min_{n \in [2,15]} |f_c - nf_0|, \tag{14}$$

with distance

$$d_g = |f_c - n^* f_0|. \tag{15}$$

The candidate is marked as potentially contaminated when

$$d_g \leq 5 \text{ Hz}. \tag{16}$$

Confidence is set low when the candidate is near a grid harmonic; otherwise confidence is based on the presence or absence of corroborating harmonics.

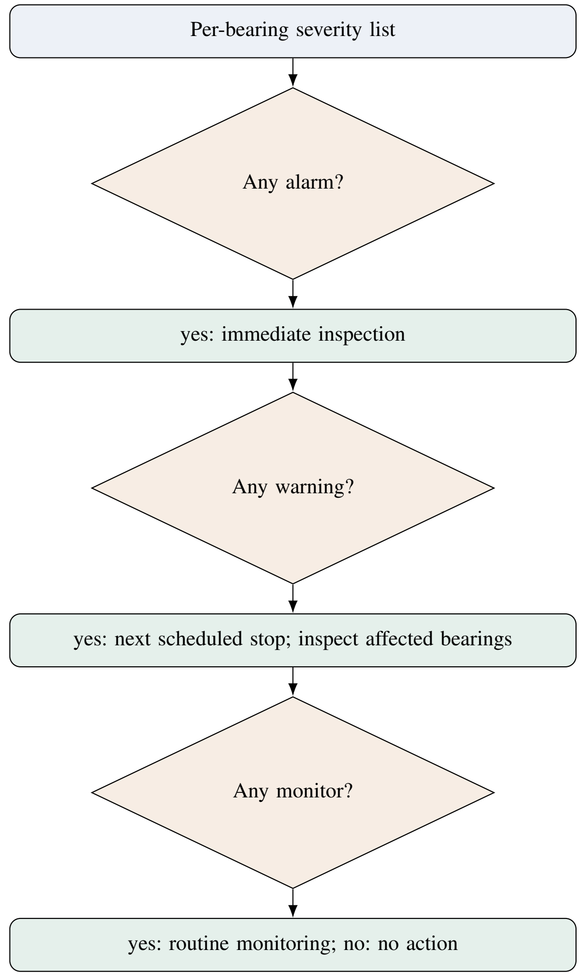

Fig. 3. Maintenance recommendation logic derived from bearing severity.

E. Maintenance Recommendation Logic

The reporting layer converts per-bearing severity into maintenance actions. The logic is conservative: alarm evidence creates immediate urgency, warning evidence creates next scheduled stop urgency, and monitor evidence creates routine monitoring recommendations.

VI. Experimental Setup and Dataset

The field dataset contains 53 captures from the Excel Valencia USMOTOR B081HC4V356 10 HP motor-pump setup. The acquisition configuration used 32 kSPS waveform data, high-resolution FFT processing, calibration files, and a bearing geometry file containing the DE and NDE bearings.

The grouped validation dataset is summarized in Table III. Group labels reflect field notes from the test campaign.

VII. Results

A. Maintenance Alerts

The final report places maintenance alerts before all numerical tables. This allows a human or automated reviewer to immediately extract required actions. Table IV summarizes the five alerts produced from the 53 captures.

TABLE III
FIELD VALIDATION GROUPS AND STATISTICAL SUMMARY.

Group	N	BRG	B_{mean}	B_{p95}	B_{max}	ROT	IMP
G0: Nut imbalance, 10 Jun	5	0	0.000096	0.000170	0.000190	0	0
G1: Original bearings, no damage	8	0	0.000080	0.000119	0.000130	0	0
G2: Original bearings plus one damaged ball	22	2	0.000622	0.005293	0.005970	15	0
G3: New bearings plus impeller imbalance	10	0	0.001289	0.005812	0.005870	4	4

TABLE IV
MAINTENANCE ACTIONS GENERATED FROM FIELD EVIDENCE.

Capture	Urgency	Action	Affected	Rationale
20260611_165656_181	next scheduled stop	inspect both	DE+NDE	Both bearings show elevated BPFO/BPFI evidence; MCSA cannot rule out either bearing.
20260611_170156_485	next scheduled stop	inspect both	DE+NDE	Both bearings show elevated BPFO/BPFI evidence; MCSA cannot rule out either bearing.
20260611_194955_561	next scheduled stop	inspect DE	DE	Drive-end bearing shows elevated BPFO/BPFI evidence; NDE remains below warning.
20260611_195442_821	next scheduled stop	inspect DE	DE	Drive-end bearing shows elevated BPFO/BPFI evidence; NDE remains below warning.
20260611_193518_553	routine monitoring	monitor	NDE	NDE shows monitor-level elevation without reaching warning.

TABLE V
REPRESENTATIVE GRID-HARMONIC CONTAMINATION CASES.

Feature	Feature Hz	Nearest harmonic	Distance
BPFO_DE	182.2	$3f_0 \approx 180$	2.23 Hz
BPFI_DE	296.3	$5f_0 \approx 300$	3.70 Hz
Blade_hi	418.9	$7f_0 \approx 420$	1.1 Hz
5HarmR low	239.8	$4f_0 \approx 240$	0.18 Hz

No capture reached the immediate category because no bearing exceeded the alarm threshold of $B_{max} \geq 0.006$. The highest observed values remained just below that boundary.

B. Harmonic Contamination Discovery

A major engineering finding was the proximity between candidate diagnostic frequencies and electrical harmonics. Table V lists representative examples.

This explains why low-resolution STFT band-energy methods may merge mechanical and electrical features. The global FFT, with $df \approx 0.122$ Hz, resolves the features, while a 4096-sample STFT with $df = 7.8125$ Hz can place these features in the same bin as a grid harmonic.

C. Interpretation

The field results support four conclusions. First, DE and NDE should not be assumed mutually exclusive; in two confirmed bearing-related captures, both bearings showed warning-level evidence. Second, harmonic corroboration adds physical interpretability without changing the original fault thresholds. Third, fifth-harmonic pump evidence is useful as confirmation but is strongly correlated with rotor-unbalance evidence. Fourth, the maintenance recommendation layer changes the output from a numerical diagnostic table into an actionable maintenance report.

VIII. DISCUSSION

The application is intentionally conservative. The added evidence fields do not modify the existing fault flags or thresholds. This separation allows the field-validated diagnostic layer to remain stable while adding explainability and maintenance value.

An attempt to apply broad band-ratio logic directly to the high-resolution global FFT was informative. The problem was not the concept of band energy, but the spectral source. High-resolution global FFTs produce narrow, resolvable lines. Integrating a wide band around these lines either adds little information or risks contamination from nearby electrical harmonics. Future persistence analysis should therefore use segmented long-window FFTs rather than low-resolution STFT bins.

IX. FUTURE WORK

A. Long-Window Temporal Persistence

Future work will split long captures into multiple large overlapping segments and compute high-resolution FFT evidence per segment. This preserves enough resolution to separate BPFO/BPFI/blade-pass from grid harmonics while enabling true temporal persistence scoring.

B. Park Vector Modulus

A complementary route based on the squared Park vector modulus will be evaluated. Using three-phase currents,

$$\begin{bmatrix} i_d \\ i_q \end{bmatrix} = \sqrt{\frac{2}{3}} \begin{bmatrix} 1 & -\frac{1}{2} & -\frac{1}{2} \\ 0 & \frac{\sqrt{3}}{2} & -\frac{\sqrt{3}}{2} \end{bmatrix} \begin{bmatrix} i_A \\ i_B \\ i_C \end{bmatrix}, \tag{17}$$

then

$$|I_s(t)|^2 = i_d^2(t) + i_q^2(t). \tag{18}$$

After removing the DC component, the demodulated signal may expose f_{mec} and Nf_{mec} components with reduced power-frequency interference.

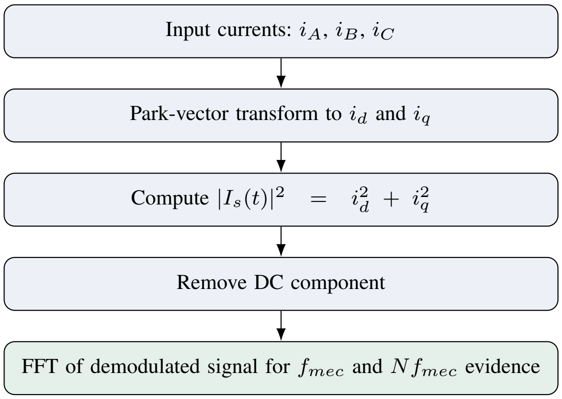

Fig. 4. Future Park-vector route for demodulated current evidence.

X. Conclusion

This paper presented a field-validated MCSA application for motor-driven centrifugal pump monitoring. The application independently evaluates multiple bearing geometries, exposes harmonic corroboration, reports fifth-harmonic pump evidence, flags grid-harmonic contamination, and converts spectral findings into maintenance actions. Validation on 53 field captures showed that five maintenance-relevant cases can be highlighted at the beginning of the report while previously validated fault thresholds remain unchanged. The result is an explainable MCSA pipeline that moves from fault indication toward maintenance decision support.

Appendix A
Mermaid Diagram Source Code

The compiled PDF uses native TikZ diagrams so the figures are visible in Overleaf without external rendering. The following Mermaid sources are included for regeneration in Mermaid-compatible tools.

A. System Architecture

```
flowchart LR
    A[ADE9000 Three-Phase Acquisition\n32 kSPS Current/
     Voltage] --> B[Raw TCP Waveform Capture]
    B --> C[Calibration + DSP Runtime Config]
    C --> D[High-Resolution Full-Band FFT]
    D --> E[Bearing Evidence\nDE + NDE]
    D --> F[Pump Evidence\nBlade Pass + 5th Harmonic]
    D --> G[Electrical Evidence\nSlip + Rotor Sidebands +
     THD]
    E --> H[Maintenance Recommendation Engine]
    F --> H
    G --> H
    H --> I[Actionable Report\ninspect_both / inspect_de /
     monitor]
```

B. Multi-Bearing Evidence Pipeline

```
flowchart TD
    A[Bearings JSON] --> B[Read all configured bearings]
    B --> C[Compute BPFO/BPFI/BSF/FTF for each bearing]
    C --> D[Extract spectral ratios from global FFT]
    D --> E[Compute Bmax = max(BPFO, BPFI)]
    E --> F[Assign severity: none / monitor / warning /
     alarm]
    F --> G[Generate bearing_flagged list]
    G --> H[Maintenance action]
```

C. Maintenance Decision Tree

```
flowchart TD
    A[Per-bearing severity evidence] --> B{Any alarm?}
    B -- Yes --> C[immediate]
    B -- No --> D{Any warning?}
    D -- Both DE+NDE --> E[next_scheduled_stop: inspect_both
     ]
    D -- DE only --> F[next_scheduled_stop: inspect_de]
    D -- NDE only --> G[next_scheduled_stop: inspect_nde]
    D -- No --> H{Any monitor?}
    H -- Yes --> I[routine_monitoring: monitor]
    H -- No --> J[no_action]
```

D. Grid Harmonic Contamination Logic

```
flowchart LR
    A[Candidate frequency fc] --> B[Find nearest n*f0, n
     =2..15]
    B --> C[Compute dg = abs(fc - n*f0)]
    C --> D{dg <= 5 Hz?}
    D -- Yes --> E[near_grid_harmonic = true\nconfidence =
     low]
    D -- No --> F[near_grid_harmonic = false\nconfidence
     from harmonic evidence]
```

E. Future Park Vector Modulus Route

```
flowchart LR
    A[IA, IB, IC] --> B[Clarke / Park Vector]
    B --> C[id, iq]
    C --> D[|Is(t)|^2 = id^2 + iq^2]
    D --> E[Remove DC component]
    E --> F[FFT of demodulated signal]
    F --> G[fmec and N*fmec evidence]
```

References

[1] H. Adaika, Z. Tir, M. Sahraoui, and K. Laadjal, “PumpSpectra: An MCSA-Based Platform for Fault Detection in Centrifugal Pump Systems,” *Sensors*, vol. 25, no. 6916, 2025.

[2] V. Becker, T. Schwamm, S. Urschel, and J. A. Antonino-Daviu, “Fault Investigation of Circulation Pumps to Detect Impeller Clogging,” *Applied Sciences*, vol. 10, no. 7550, 2020.

[3] S. Singh, A. Kumar, and N. Kumar, “Motor Current Signature Analysis for Bearing Fault Detection in Mechanical Systems,” *Procedia Materials Science*, vol. 6, pp. 171–177, 2014.

[4] P. Popaleny, A. Duyar, C. Ozel, and Y. Erdogan, “Electrical Submersible Pumps Condition Monitoring Using Motor Current Signature Analysis,” SPE Artificial Intelligence and Advanced Analytics, Paper 193081, 2018.

[5] Y. Han, J. Zou, A. Presas, Y. Luo, and J. Yuan, “Off-Design Operation and Cavitation Detection in Centrifugal Pumps Using Vibration and Motor Stator Current Analyses,” *Sensors*, vol. 24, no. 3410, 2024.